Electronic Supplementary Material (ESI) for RSC Advances.

Supporting Information

Directional design of carboxylic acid coordination number fine-tuned space structure to improve the output performance of nanogenerators

Yong-Juan Zhou[b], Shi-Hui Wang[b] , Zi-Kun Zhang [b] , Jiabin Xiong [a,b*]

[a.]College of Chemistry, Green Catalysis Center, International Phosphorus Laboratory, International Joint Research Laboratory for Functional Organophosphorus Materials of Henan Province, Zhengzhou University, Zhengzhou 450001, People's Republic of China. E-mail: xjiabin@foxmail.com.

[b.]School of Material and Chemical Engineering, Center for Advanced Materials Research, Zhongyuan University of Technology, Zhengzhou, 450007, China.

Table of Contents

1.Experiments

1.1 Materials

The chemicals and reagents involved in this experiment were obtained by purchasing through commercial platforms and were used directly without further purification.

1.2 Synthesis of compounds **1-2**

Synthesis of [Zn (HTCPE)] (**1**). $Zn(NO_3)_2$-$6H_2O$ (16.06 mg, 0.054 mmol), H_4TCPE (8 mg, 0.009 mmol) and 4,4'-bipyridine (3 mg, 0.017 mmol) were dissolved in a mixture of methanol (0.5 mL), DMF (2 mL), and 10 μL (1 M) hydrochloric acid. The mixed solution was then placed in a 10 mL reactor and heated in a programmable oven that was preheated to 110 °C for 48 h, and then cooled to room temperature at a rate of 5 °C h^{-1} to obtain light yellow Zn-MOF [Zn(HTCPE)] crystals. These crystals obtained were washed with excess DMF and methanol and dried at room temperature.

Synthesis of [Cu_4(ETTB)] (**2**). $Zn(NO_3)_2$-$6H_2O$ (15 mg) was dissolved with H_8ETTB (5 mg) in a solution of N,N-diethylformamide (1.6 mL), and the resulting mixed solution was placed in a 5 mL heat-resistant vial, followed by the addition of 1 drop of fluoboric acid. The mixed solution was placed in an oven preheated to 75ºC for 96 h and then cooled to room temperature at a rate of 5°C h^{-1} to obtain colorless Zn-MOF [Zn (H_8ETTB)] crystals. The Zn-MOF[Zn (H_8ETTB)] crystals were washed with appropriate amount of DMF and methanol and dried at room temperature. Colorless crystals of Zn (H_8ETTB) (5 mg) and $Cu(NO_3)_2$ $2.5H_2O$ (15 mg) were taken and added to 1.6 mL of N,N-dimethylformamide, and the resulting mixture was placed in a 5 mL heat-resistant vial, and the mixture was stored at room temperature for 4 days to obtain green crystals of [$Cu_{4(}$ETTB)]. The obtained green crystals were washed with excess DMF and methanol and dried at room temperature.

1.3 Preparation of 1/2 base TENG

TENG positive electrode sheet preparation: the compound **1** and **2** grinding evenly coated in 5cm × 6cm copper sheet, and will be coated with conductive silver epoxy resin of the copper wire fixed in the other side of the copper sheet, in the fixed copper wire of the copper tape surface covered with a layer of transparent adhesive tape, and finally cut it out into 5cm × 5cm.

TENG negative electrode sheet (PVDF) preparation: weighing the appropriate amount of PVDF powder dissolved in a mixture of DMA and acetone, stirring at 60 ℃ until the PVDF completely dissolved to stop the heating, cooled to room temperature, through the desktop homogenizer will be uniformly coated with the PVDF mixture on the Kapton membrane, the spin-coating of the membrane is placed in the oven drying at 80 ℃ for 4 h and then remove the cooled to room temperature. room temperature. A copper tape of 5 cm × 6 cm was applied to the reverse side of the PVDF film, and the negative electrode sheet was prepared in the same way as the positive electrode sheet.

2.Working principle of assembling TENG

Fig. S4i represents the initial state of the potential difference of the external circuit without external force; when a certain external force is applied, the two electrodes are in contact with each other, and an equal number of charges but with opposite signs will be generated in the PVDF and compound layers, and the PVDF layer is negatively charged with respect to the compound electrode layer (ii); when the external force is removed, the potential difference between the upper and lower electrodes will be generated due to electrostatic induction (iii), and the potential difference will disappear when the The potential difference disappears when the charge reaches equilibrium again (iv); when the same external force is applied to the TENG system again, the distance between the two layers of electrode material changes again, which causes the potential difference between the two electrodes to change as well (the potential difference decreases with the decrease of the distance), and thus the electrons flow from the PVDF electrode to the compound layer (Fig. V), until the charge accumulates to reach the new charge equilibrium (ii).

3. Characterization

Thermogravimetric analysis (TGA) data were collected on a Netzsch STA 449C thermal analyzer. The compounds were subjected to Mott - Shottky test by a three-electrode system on an electrochemical workstation (CHI 660E, Shanghai Chenhua Instrument Co., Ltd., China). The chemical bond determination of the compounds was tested by FT-IR; the purity was characterized by powder X-ray diffraction mapping (PXRD) under Cu-kα irradiation using an instrument manufactured by Bruker D8 Advance. For testing the elemental composition and valence states XPS was used to obtain spectral data plots of the compounds

using Al-Kα as the ray source. The morphology, elemental composition and distribution of the compounds were tested with a German-made FE-SEM and its accompanying EDS. The Isc and Voc of the friction nanogenerators were tested at the SR570 low-noise current amplifier (Stanford Research Systems) and at the 2657A high-power system source table.The bandgap sizes of the samples were tested with the UV-2600 UV-visible diffuse reflectance spectrometer.

The electrolyte for the Mott - Shottky test was Na2SO4 solution at a concentration of 0.2 mol/L. The three-electrode system had the counter electrode connected to a Pt electrode, the reference electrode was an Ag/AgCl electrode, and the working electrode was connected to a conducting glass loaded with compounds 1 and 2. The tests were carried out with the Impedance-Potential module in the Shanghai Chenhua electrochemical workstation with the voltage test range of -1-1 V and the test frequencies of 500 Hz, 1000 Hz, and 1500 Hz.

The crystal structure is determined by X-ray single crystal diffractometer, and the crystal structure can be solved. In this experiment, we mainly used the D 8venture model of Bruker, USA, and mainly synthesized single crystals for structural analysis. The test target is molybdenum target, the temperature is 298k, the voltage is 50kv, the use of Mo-K α -ray. The single crystal structure was mapped by Diamond Software.

4. Diagrams

Table S1. Crystallographic data and structure refinement parameters for compounds **1**-**2**

Complex	1	2
empirical formula	$C_{54}H_{41}Zn_{1.05}O_8 \cdot (C_2H_8N)$	$Cu_4C_{58}H_{28}O_{20}$
crystal system	monoclinic	tetragonal
space group	$P2_1/c$	I4/mmm
a[Å]	10.1691(4)	18.583(16)
b[Å]	10.1917(4)	18.583(16)
c[Å]	42.7903(18)	35.68(3)
α[°]	90	90
β[°]	92.925(2)	90
γ[°]	90	90
V[Å^3]	4429.03(30)	12321.3(190)
Z	4	4
ρ_{calc} (g cm^{-3})	1.423	0.700
μ [mm^{-1}]	1.288	0.716

GOF(F^2)	1.119	1.053
R_1	0.1040	0.0902
wR_2	0.2722	0.2621

[for 7779 data I > 2σ(I)]

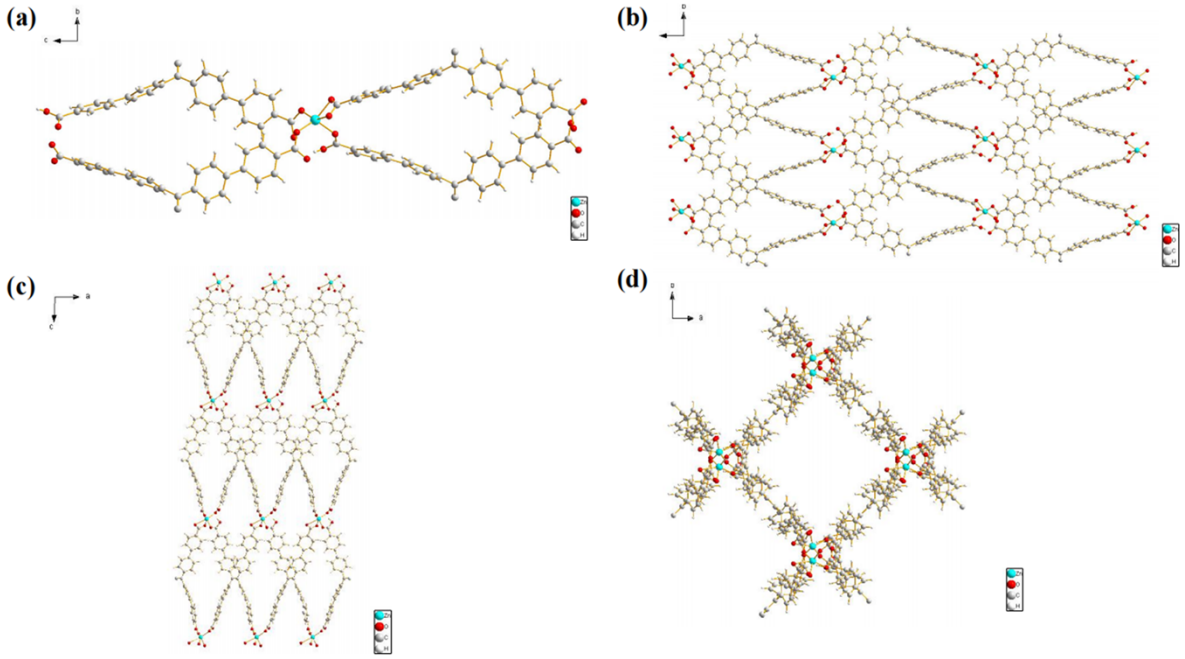

Figure. S1 Perspective view of Zn-MOF crystal structure (a) complex structure of Zn-metal node (b) crystal structure of Zn-MOF along crystallographic a-axis, (c)b-axis, and (d)c-axis. C, gray; O, red; Zn, blue; H, white.

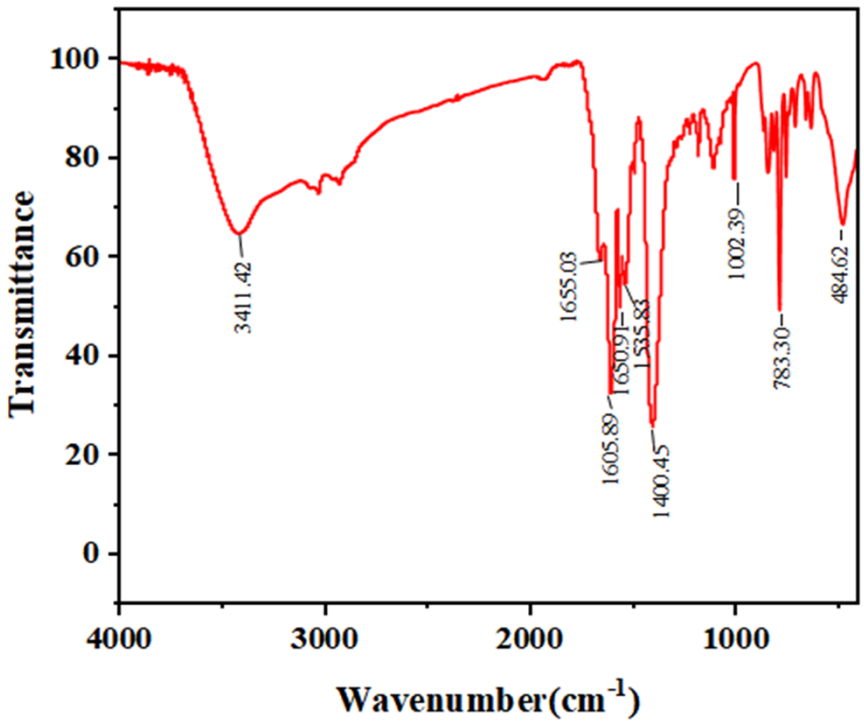

Figure. S2 FT-IR of compound **1**.

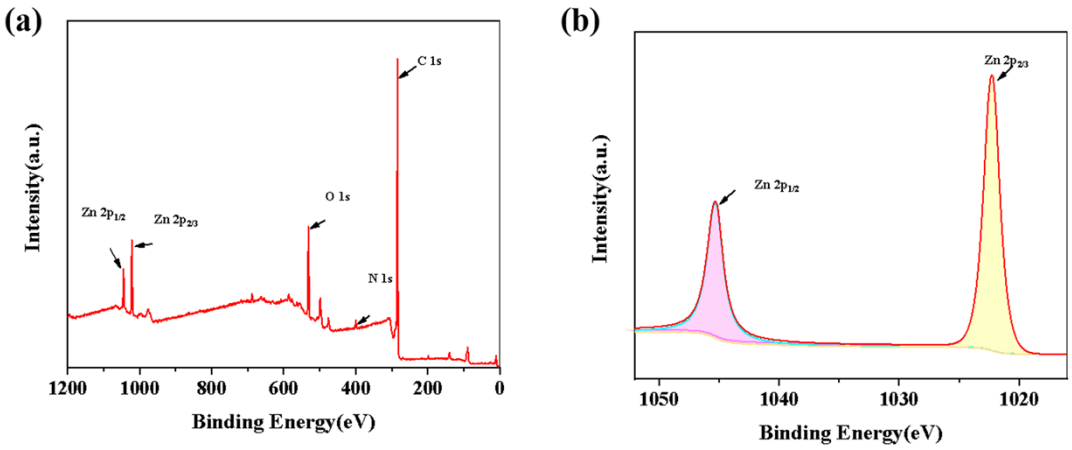

Figure. S3 (a) XPS full spectrum of compound **1**; (b) XPS profile of Zn ion in compound **1**

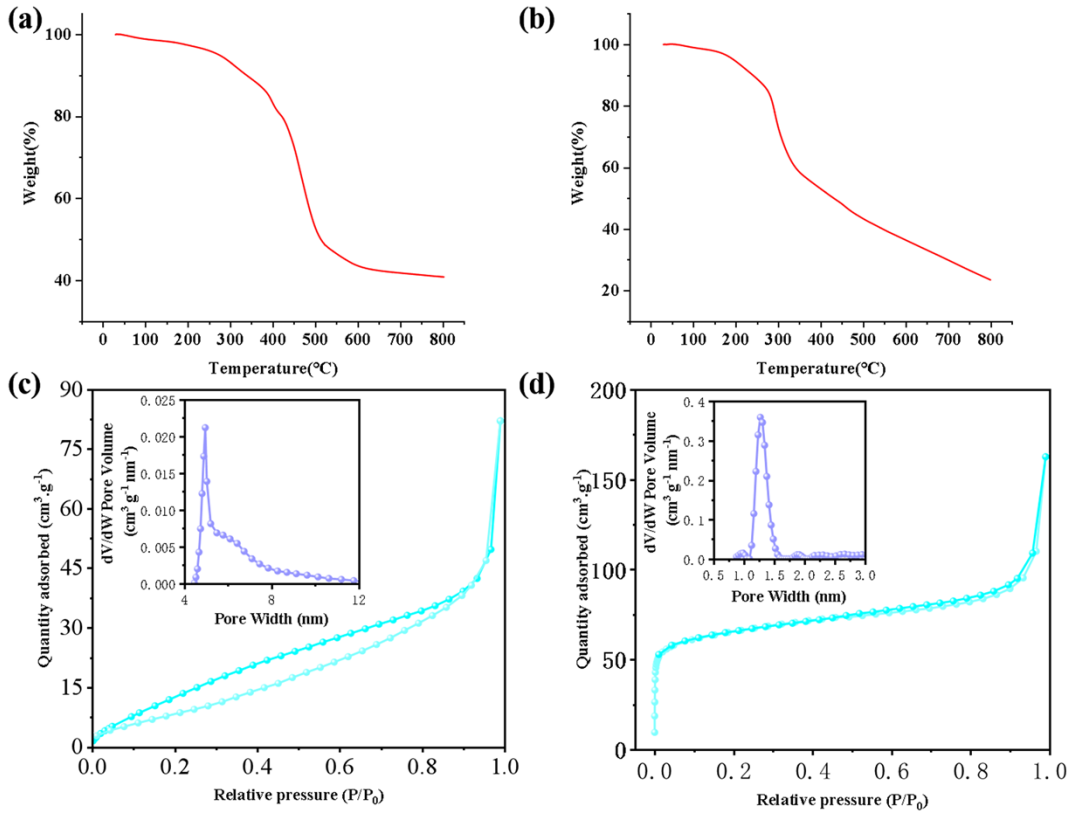

Figure S4 (a-b) TGA of compounds **1** and **2**; (c-b) N_2 adsorption-desorption isotherms of compounds **1** and **2**.

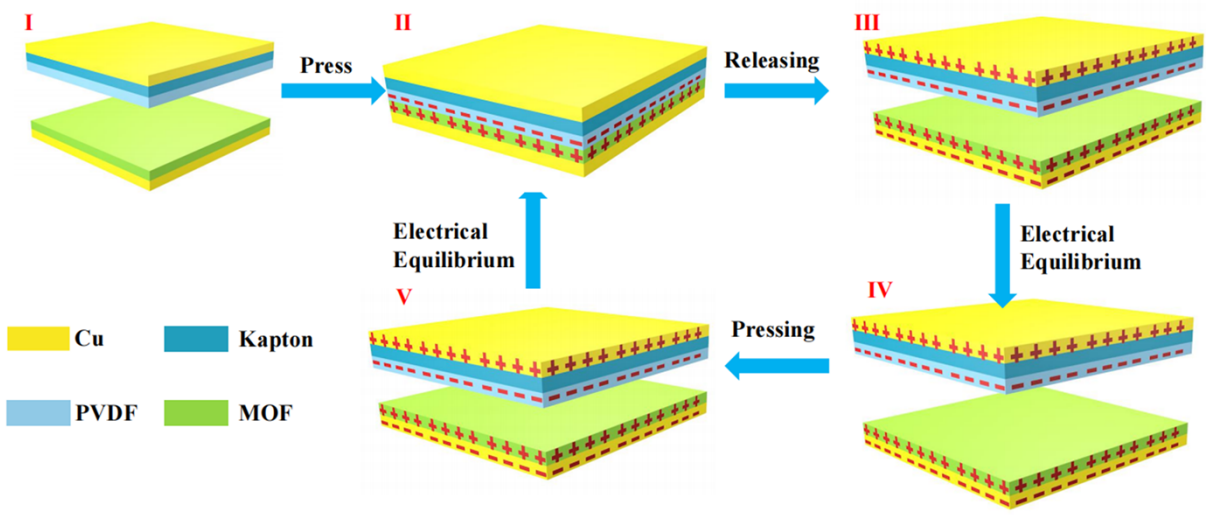

Figure. S5 Mechanism diagram of TENG device operation.

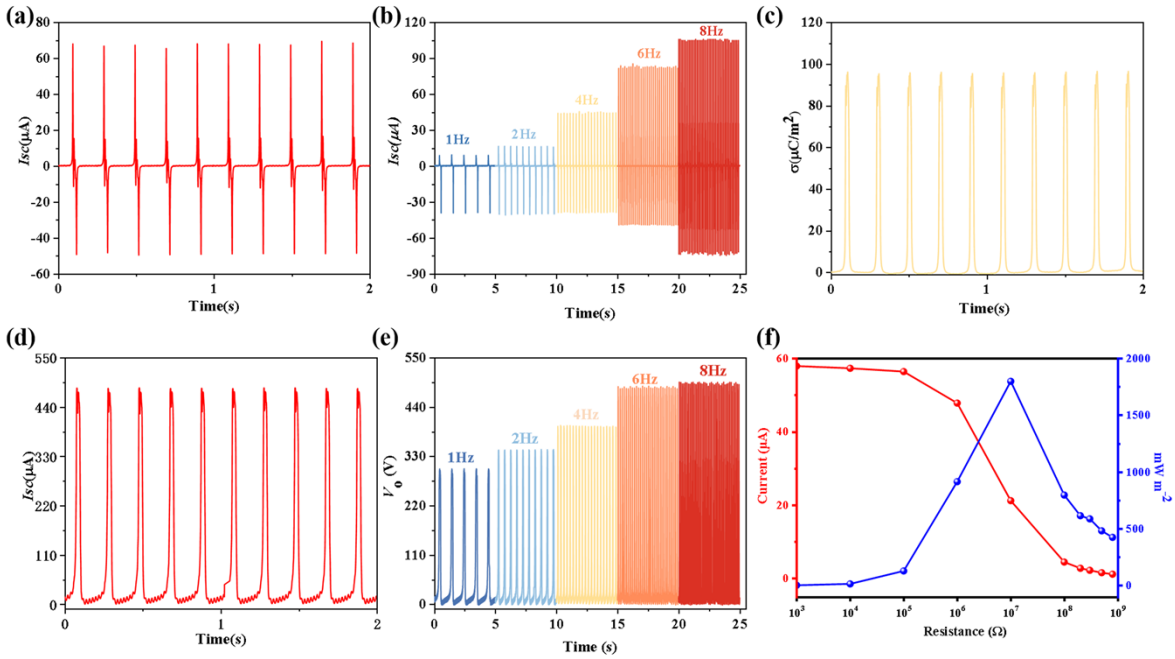

Figure. S6 (a) Isc, (c) σ, (d) Voc, (f) **1**-TENG power density at 5 Hz; (b), (e) Isc vs. Voc for **1**-TENG at different frequencies from 1 to 8 Hz.

A frictional power generator 1-TENG was made for testing under the same test conditions using 1 as the electrode material. When 1 was operated at 5 Hz, the peak values of short-circuit current and open-circuit voltage were 68.23μA (Fig. a) and 485.32 V (Fig. d), and the charge density was96.24 μC m-2 (Fig. c). Depending on the power density and short-circuit current of the friction nanogenerator at different load resistances, the instantaneous power reaches a peak of 1806.36 mW m-

2 when the load resistance is 10 MΩ (Fig. f). As shown in Figs. b and e, the output performance of the TENG, Isc and Voc, increases gradually with increasing frequency, reaching 105.86 μA and 493.90 V at 8 Hz.

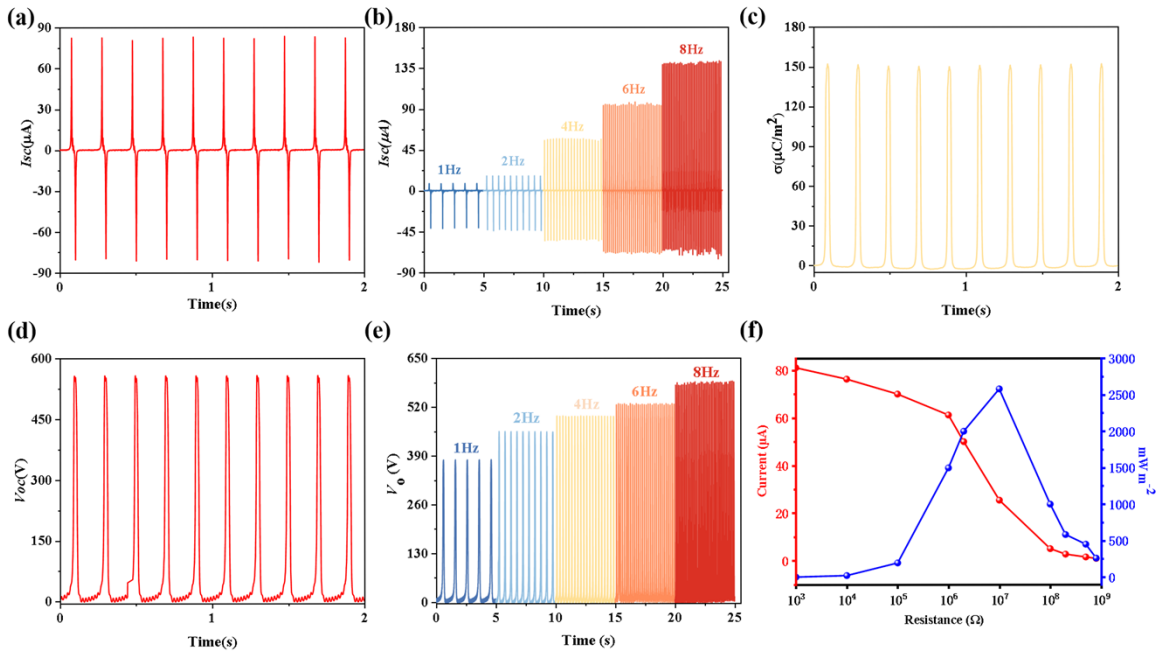

Figure. S7 (a) Isc, (c) σ, (d) Voc, (f) **2**-TENG power density at 5 Hz; (b), (e) Isc vs. Voc for **2**-TENG at different frequencies from 1 to 8 Hz.

A frictional power generator 2-TENG was made for testing under the same test conditions using 2 as the electrode material. When 2 was operated at 5 Hz, the peak values of short-circuit current and open-circuit voltage were 84.49μA (Fig. a) and 560.45 V (Fig. d), and the charge density was151.99 μC m-2 (Fig. c). Depending on the power density and short-circuit current of the friction nanogenerator at different load resistances, the instantaneous power reaches a peak of 2594.93 mW m-2 when the load resistance is 10 MΩ (Fig. f). As shown in Figs. b and e, the output performance of the TENG, Isc and Voc, increases gradually with increasing frequency, reaching 140.35 μA and 583.43 V at 8 Hz.

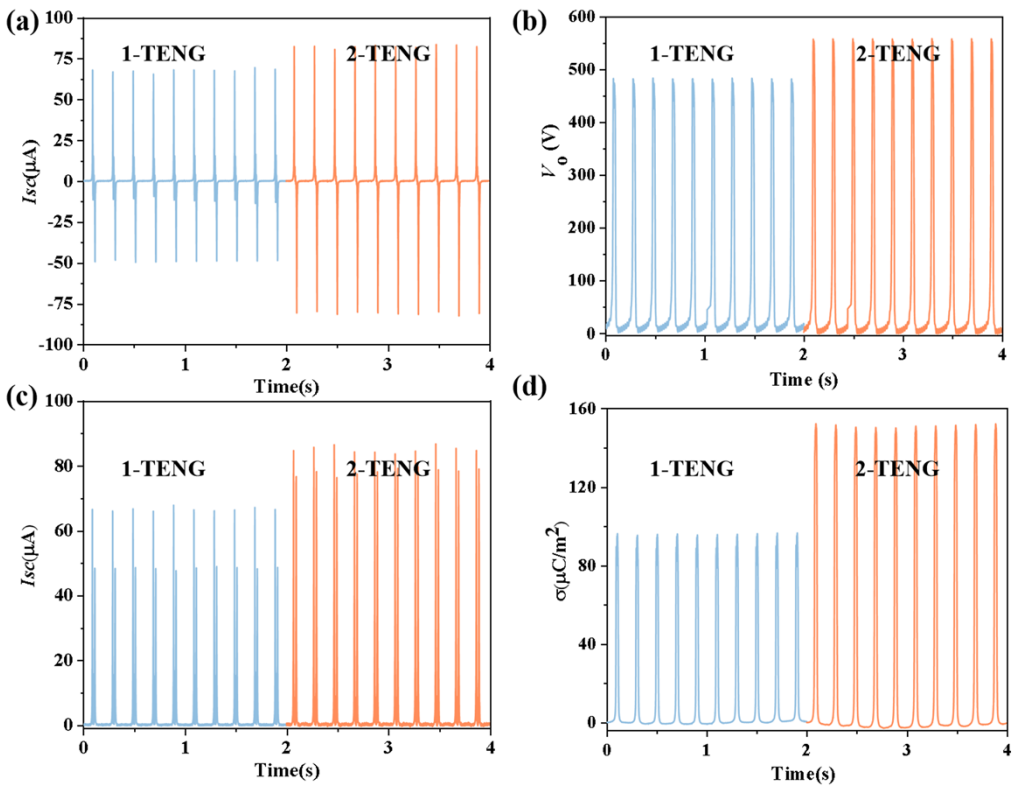

Figure. S8 Comparison plots of **1**-,**2**-TENG at 5 Hz (a) current comparison , (b) voltage comparison, (c) rectification comparison, (d) charge density comparison.

The short-circuit current (Isc) and output voltage (Vo) of 1-, 2-TENG at 5 Hz were 68.23μA and 485.32 V, 84.49 μA and 560.45 V, respectively. The rectifying and charge densities (σ) were 66.55 μA and 96.24μC m-2,84.41 μA and 151.99 μC m-2, respectively.

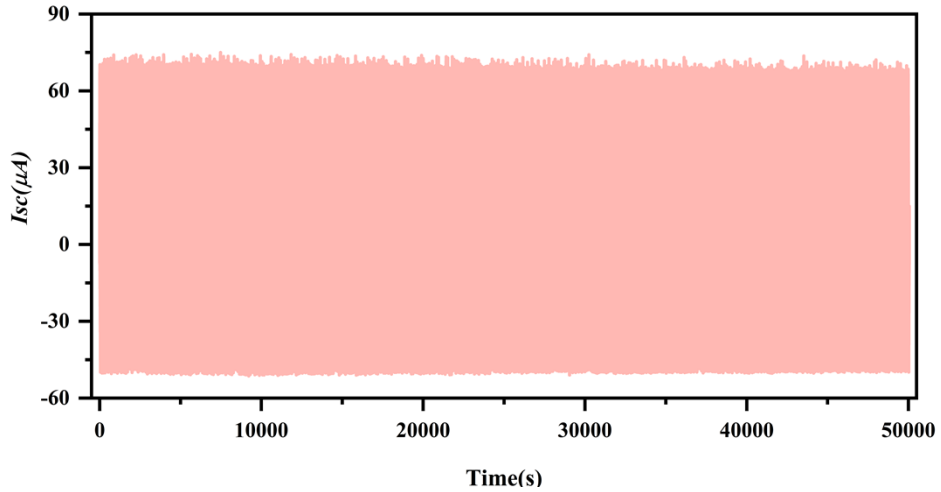

Figure. S9 Isc of **1**-TENG after 50,000 cycle

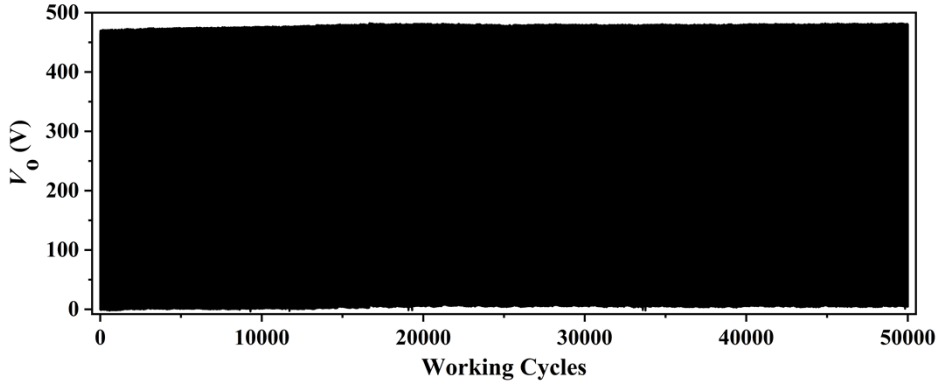

Figure. S10 1-TENG Isc after 50,000 cycles.

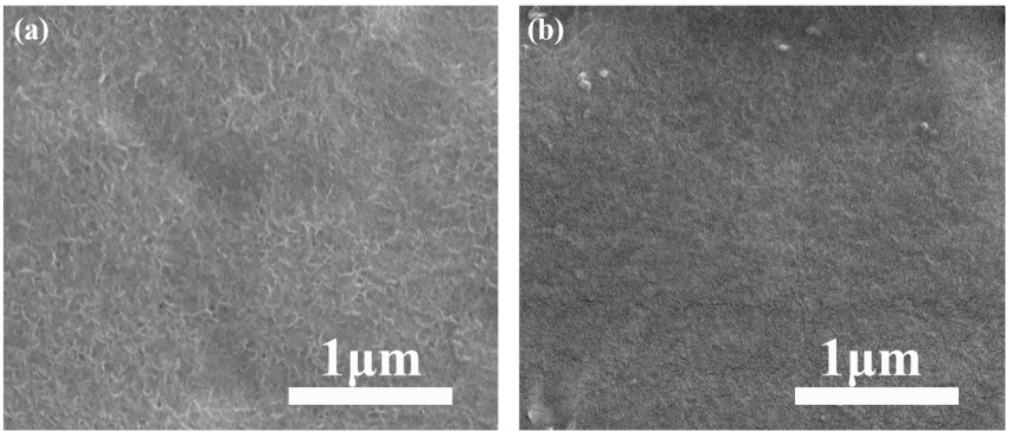

Figure. S11 (a) FE-SEM image of PVDF before testing; (b) FE-SEM image of PVDF after testing.

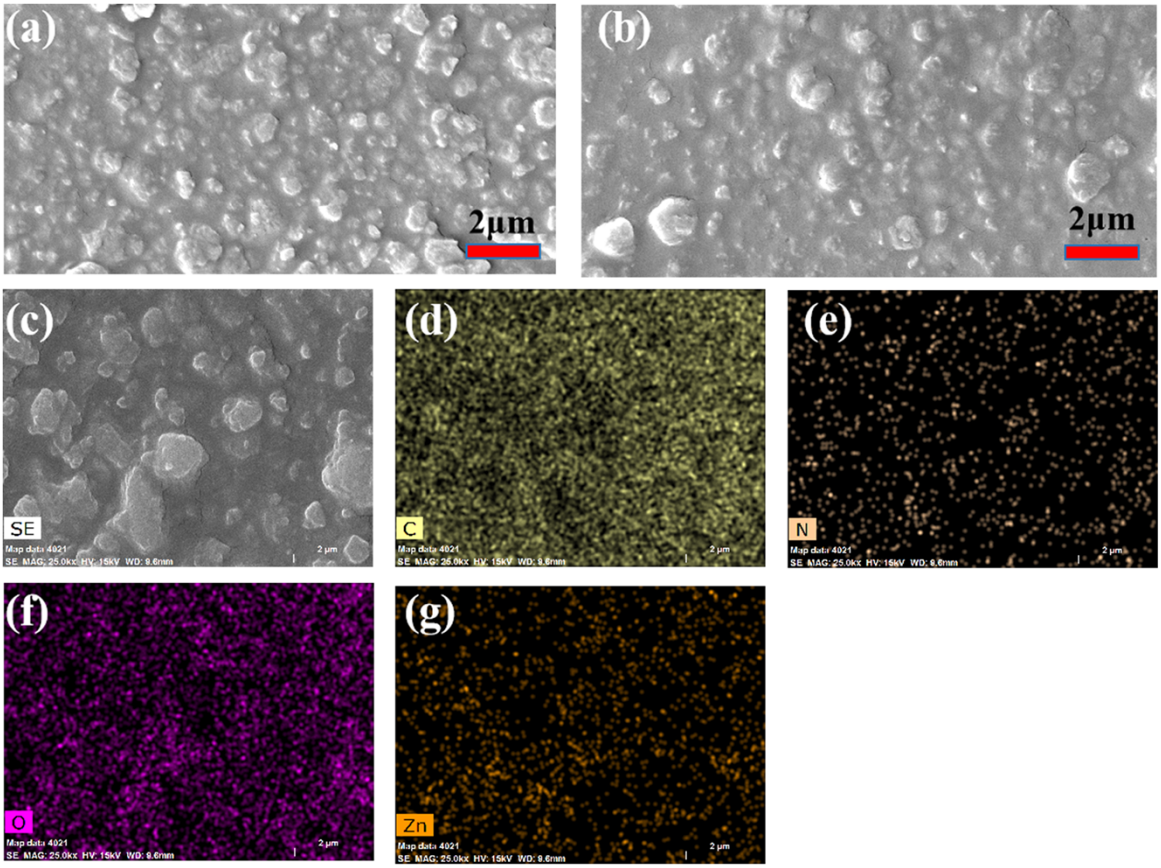

Figure. S12 (a) FE-SEM image of compound **1** before testing; (b) SEM image of compound **1** after testing; (c-h) EDX-mapping analysis of each element in compound **1**.

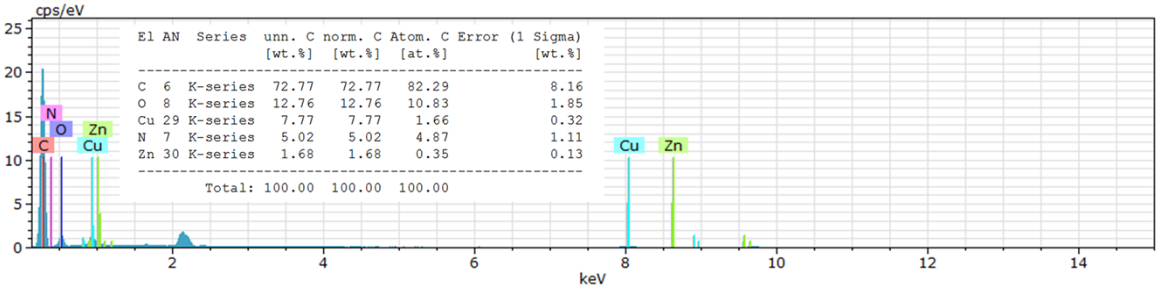

Figure. S13 The EDX-mapping of Zn element in compound 2

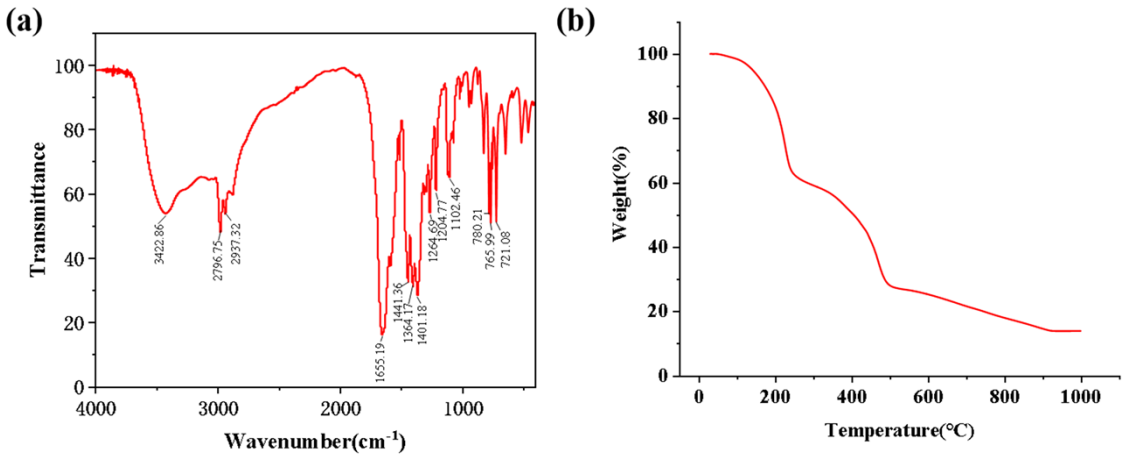

Figure. S14 Infrared and thermogravimetric of Zn(H8ETTB)

Table S2. Literature data were compared

Analytes	Methods	Reference	Test Current（μA）
MOF	TENG	Journal of Materials Chemistry C，9（2021），17319-17330	Compound**1**/**2**/**3**=1.7 mA/0.3 mA/0.17 mA
	TENG	ACS Appl Mater Interfaces，14（2022），16424-16434	Compound**1**/**2**/**3**=31.32 μA/45.69 μA/68.82 μA
	TENG	Angew. Chem. Int. Ed，4（2022），e202208994	Compound**1**/**2**/**3**=53.08μA /84.53μA/97.03 μA
	TENG	Nano Energy，45（2018），420-431	220μA
	TENG	This work	Compound**1**/**2**=68.23μA/85.17μA